Journal of Structural Geology 32 (2010) 394–406

Contents lists available at ScienceDirect

Journal of Structural Geology

journal homepage: www.elsevier.com/locate/jsg

# Structural evolution of the Northern Cerberus Fossae graben system, Elysium Planitia, Mars

Joyce Vetterlein*, Gerald P. Roberts

*The Research School of Earth Sciences at Birkbeck and University College London, Gower Street, London, WC1E 6BT, UK*

ARTICLE INFO

*Article history:*
Received 25 September 2009
Accepted 6 November 2009
Available online 6 January 2010

*Keywords:*
Mars
Cerberus Fossae
Graben
Normal faulting
MOLA
Palaeo-tips

ABSTRACT

To determine whether the structural evolution of the Northern Cerberus Fossae (NCF) was dominated by cryospheric melting and collapse or fault-related subsidence, we used MOC, THEMIS and HiRISE images, and MOLA data to document spatial variations in vertical offset along strike. The Fossae are a series of fractures on the martian surface that cross-cut Noachian, Hesperian and, in places, very young Late Amazonian terrain. Serial cross sections across the fracture-related topography, from MOLA data, show that vertical offsets are not greater where fractures traverse older terrain, showing that offsets have accumulated since the formation of the Amazonian terrain. Vertical offsets are greater in the central portions of the fracture system with the profile resembling that for a single fault system. Topographic features that pre-date deformation are preserved on the graben floors suggesting little sediment infill, so the MOLA elevation measurements constrain total vertical offsets since the fractures formed. Deficits in vertical offset occur where fractures have not linked and remain en echelon across relay zones, or have linked, leaving palaeo-graben-tips. This indicates that the traces of the fractures propagate along strike at the surface and intersect over time periods that are likely to be in the range of $10^5$–$10^6$ years rather than in a single collapse event. Deficits are also in places associated with collapse pits, suggesting such collapse is the early stage of graben subsidence at propagating lateral graben-tips. We use these observations to argue that the primary mechanism causing subsidence is not cryospheric melting and collapse, but faulting.



## 1. Introduction

Cerberus Fossae are a series of fractures and depressions that cross-cut one of the youngest surfaces on Mars (Fig. 1a). Debate exists concerning their mode of formation. It has been suggested that cryospheric melting and collapse associated with dike intrusion beneath the Southern Cerberus Fossae dominated local subsidence (Head et al., 2003). In this scenario, melting around a dike resulted in the emergence of large volumes of meltwater onto the martian surface, cutting the Athabasca Valles outflow channel in the last few percent of martian history (Burr et al., 2002; Berman and Hartmann, 2002; Head et al., 2003; Plescia, 2003; Keszthelyi et al., 2007). The volume of meltwater and the extent of subsidence have been linked in that the collapsed depression along the dike is thought to have filled with meltwater before overspilling to form the Athabasca Valles outflow channel (Keszthelyi et al., 2007). This implies that the subsidence occurred synchronously with melting and filling of the depression, over a timescale similar to that of dike intrusion. These features have been described predominantly for the Southern Cerberus Fossae; relatively-few observations of the Northern Cerberus Fossae exist in the literature. However, the two structures are similar in morphology and probably formed through the action of similar processes.

In this paper we investigate the possibility that, for the Northern Cerberus Fossae, subsidence is mainly the result of faulting, perhaps above a dike(s), and is not dominated by collapse due to melting of the cryosphere above and around a dike (Figs. 1–8). In this scenario, faulting occurred over millions of years through incremental fault-slip instead of over the timescale of a single dike emplacement episode. We investigate this possibility by studying the detailed geometry of the subsided graben using a variety of images (MOC, THEMIS and HiRISE images; see Section 3), and quantifying the subsidence using topographic data from an orbiting laser altimeter (MOLA). We demonstrate the following for the Northern Cerberus Fossae: (1) topographic features formed prior to graben formation have been offset by graben-faulting and can be identified on the graben floor, revealing that the depressions have not been infilled or

* Corresponding author. Tel.: +44 1424 428791.
*E-mail address:* joyce_vetterlein@hotmail.co.uk (J. Vetterlein).

0191-8141/$ – see front matter © 2009 Elsevier Ltd. All rights reserved.
doi:10.1016/j.jsg.2009.11.004

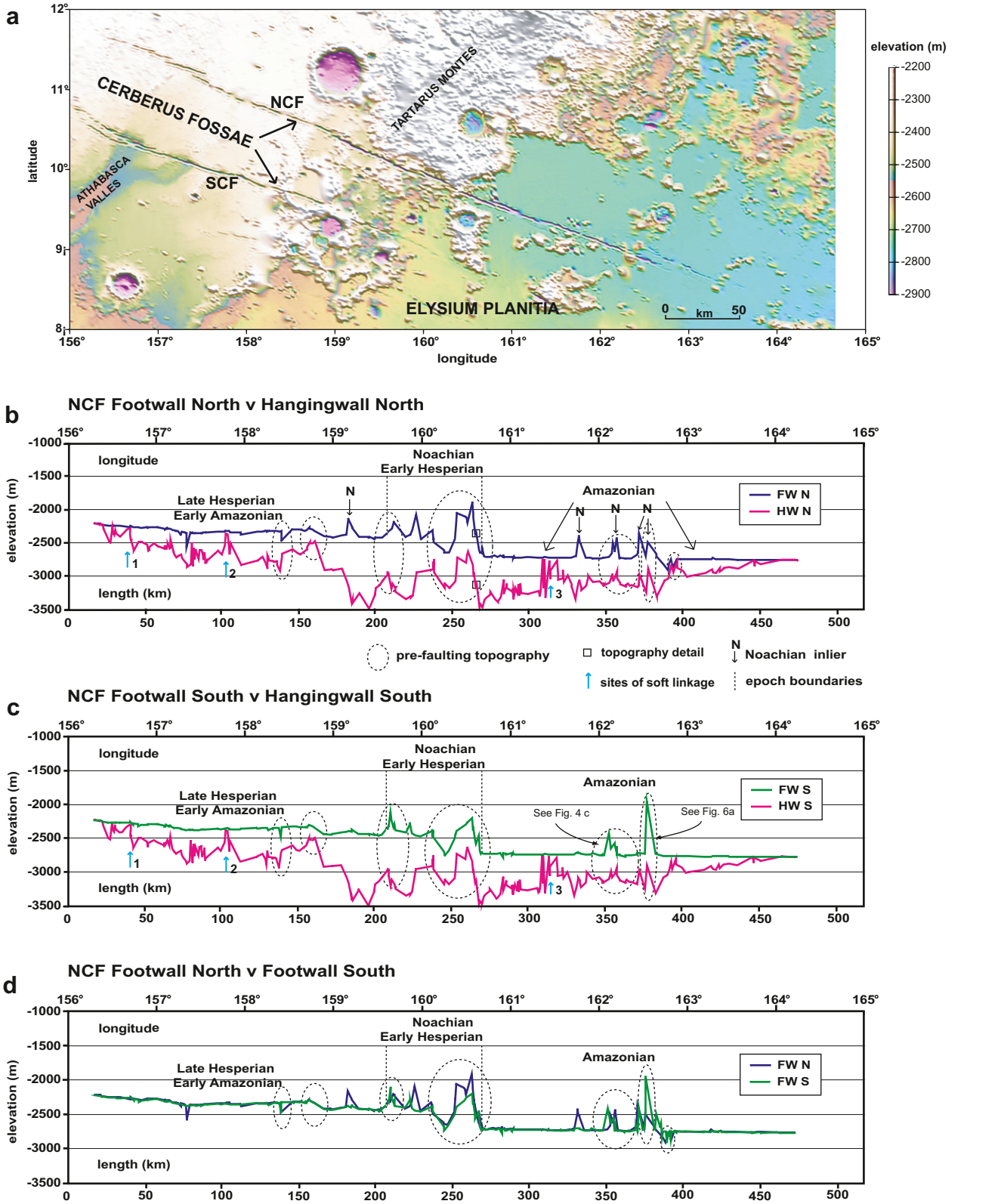


**Fig. 1.** (a) DEM of the Cerberus Fossae from MOLA data. (b), (c) and (d) Elevation data from MOLA constraining offsets across the Northern Cerberus Fossae (NCF). Data were extracted from polar Mars Global Surveyor spacecraft orbits that traversed the NCF. The elevations were taken from the floors of the graben and the crests of the north and south walls of the graben. Elevations are relative to the Mars datum; zero elevation on Mars is the elevation where atmosphere pressure is 6.1 mmillibars. (b) North wall of the graben; plot of footwall (FW N) and hangingwall (HW N) elevations against position along the graben, showing preservation of pre-faulting topography in the downthown block. (c) As (b) for the south wall of the graben. (d) Plot of both footwalls. Martian epoch chronology is from (Hartmann, 2007). Arrows show peaks in the hangingwall (HW) trace that occur at locations of graben linkage. Dashed ellipses locate examples of preserved pre-faulting topography.

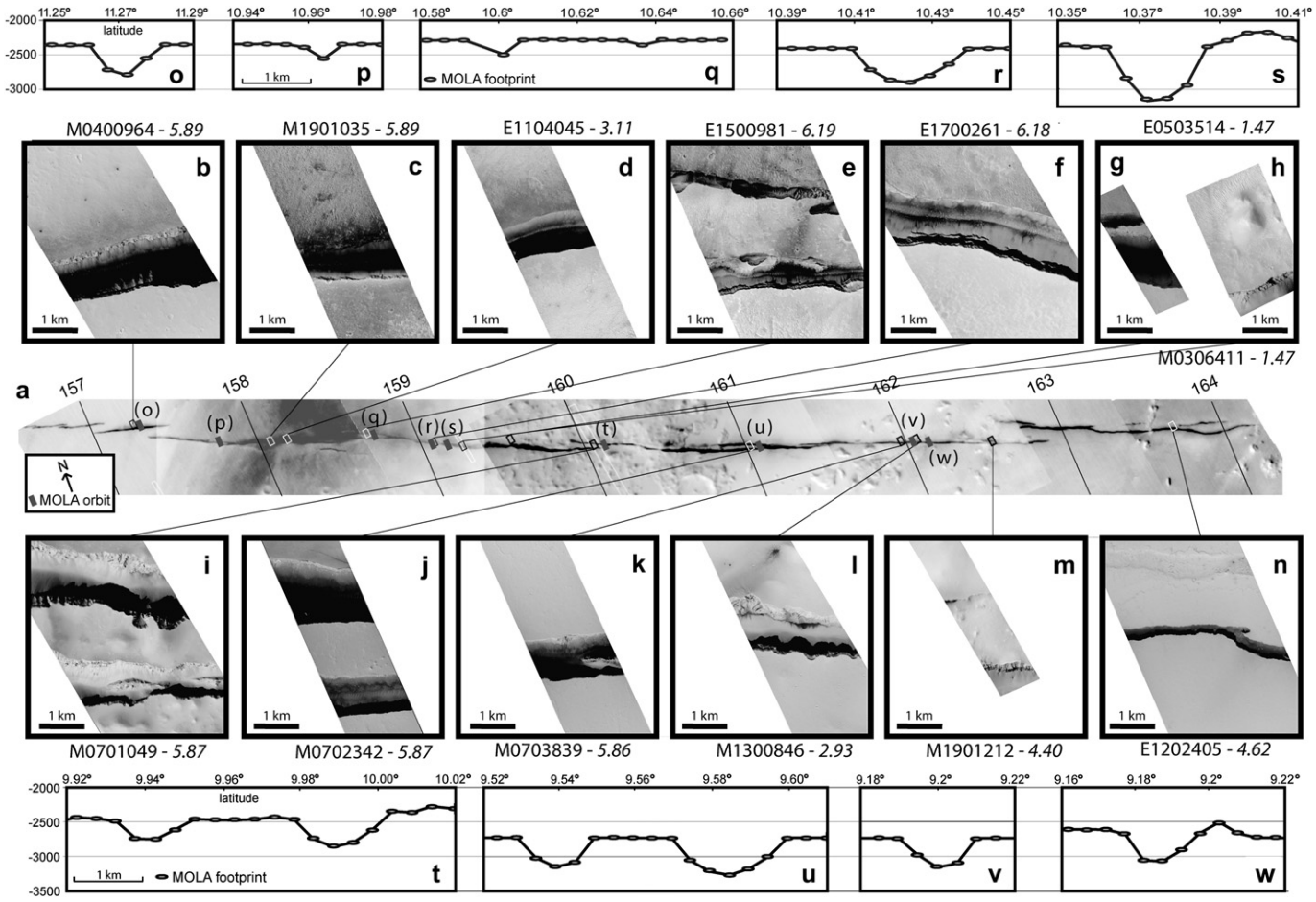


**Fig. 2.** (a) Mars Global Surveyor MOC Wide Angle image (WA) mosaic of the Northern Cerberus Fossae (NCF) rotated, with longitude east +ve. marked. (b)–(n) Numbered MOC Narrow Angle (NA) images of sections of the NCF, giving pixel dimensions (*italics*) in metres. (o)–(w) MOLA topographic traverses from polar Mars Global Surveyor spacecraft orbits. MOLA footprints are drawn to the correct horizontal scale. The difference in elevation between the floor of the graben and the crests of the north and south walls are taken to be the throws on the faults; these values are used in Figs. 1, 3 and 4.

disrupted by significant amounts of sediment or material from melting-related collapse; (2) elevation changes across graben walls are a measure of fault-related throw; (3) fault-related subsidence can be related to graben length via throw/length ratios (values between 0.1 and 0.001), and are similar to those on Earth; (4) subsidence deficits are related to structural geometry, occurring at present-day and palaeo-fault tips, implying that graben subsidence has accumulated through time via repeated fault offsets, with throw profiles controlled by the graben growth-linkage process; (5) the rates of faulting needed to produce the observed subsidence of surfaces dated by crater counting are not unreasonable (throw-rates of 0.001–1.0 mm/yr), given that they fall within the range of values known for faults on the Earth, implying that the graben formed over millions of years.

First, we give a geological background to the region, before using image mosaics and a DEM from MOLA data to map the surface expression of Cerberus Fossae in detail. Then, we use MOLA data to quantify the vertical offsets across graben walls of the NCF. We use this information to interpret the evolution of the structures.

## 2. Geological background

The Cerberus Fossae are a series of sub-parallel, linear fractures and depressions across Elysium Planitia, Mars, the largest of which form two long, segmented arrays, which will be referred to as the Northern Cerberus Fossae (NCF) and Southern Cerberus Fossae (SCF) (Fig. 1a.). The Fossae cross-cut terrain of different ages (Tanaka et al., 2005). In the west they cut Elysium lava flows of Late Hesperian to Early Amazonian age (3.2–2.0 Ga, Hartmann and Neukum, 2001). At their centres, the fossae cut through the heavily cratered Tartarus Montes region (dated Early Noachian to Early Hesperian; 4.1–3.5 Ga, Hartmann and Neukum, 2001). At the eastern end of the region we study the Fossae offsetting Late Amazonian Cerberus lavas. The suggested ages of the youngest lavas offset by Cerberus Fossae, assessed by crater counting methods, are <10 Ma (Hartmann and Berman, 2000), <10 Ma (Hartmann and Neukum, 2001), <200–20 Ma (Berman and Hartmann, 2002), <24 Ma (Fuller and Head, 2002). Vaucher et al. (2006) used a statistical method to refine crater counting dates, taking into consideration the work of McEwen et al. (2005). McEwen et al. (2005) had cast doubt on all previous crater counting ages by recognising that many small craters were secondary to the Zunil impact ~100 km east (grid ref. ~165.85°E 7.7°N) of the NCF. They concluded that the most recent age for the Athabasca Valles (Fig. 1a.), which incise the Cerberus lavas, could not be constrained to closer than 1.5–200 Ma. However, Vaucher et al. (2006) give an age for the most recent lavas as <10 Ma. <10 Ma is the age marked on the USGS Map 2888 and reported in the accompanying Pamphlet (Tanaka et al., 2005). Overall, because they cut and displace lavas of Elysium Planitia, the Fossae are amongst the youngest structures on the martian surface (<200–1.5 Ma) (Head et al., 2003).

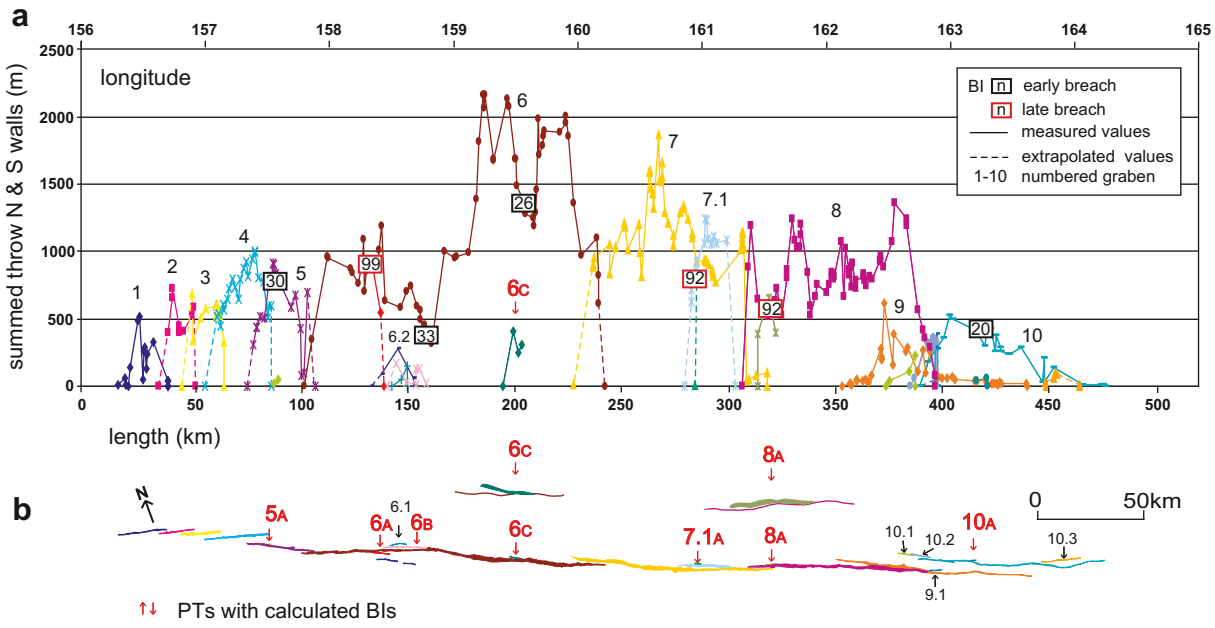


**Fig. 3.** Throw and length data for individual graben associated with the Northern Cerberus Fossae. Data for the north and south walls are summed, but are symmetrically distributed between the north and south walls in most cases. (a) Length (longitude) versus summed throw plots of individual numbered graben derived from MOLA data. Breaching indices (BI) of numbered palaeo-tips are shown. BI values in the small black and red boxes are for early and late breaching respectively. (b) Rotated map view of the graben and palaeo-tips, using latitude and longitude MOLA points, compared with THEMIS mosaic in Fig. 4. Detail of palaeo-tips 6C and 8A are shown with a factor of 5 enlargement. (For interpretation of the references to color in this figure legend, the reader is referred to the web version of this article).

The published material on the nature and formation of the Cerberus Fossae has focussed on the Southern Cerberus Fossae, the suggested water source for the Athabasca Valles floodwaters (Fuller and Head, 2002; Berman and Hartmann, 2002; Burr et al., 2002; Plescia, 2003; Jaeger et al., 2007; Keszthelyi et al., 2007). Intrusion of dikes that are radial to the Elysium Mons volcano are thought to have melted sub-surface ice deposits leading to catastrophic discharges of meltwater at the surface (see McKenzie and Nimmo, 1999 for quantification of cryospheric melting related to dike emplacement on Mars). Estimates of the aqueous discharge needed to form Athabasca Valles, given that liquid water is unstable at the low atmospheric pressures on Mars, are $1–2 \times 10^6\ m^3\ s^{-1}$ (see Head et al., 2003), and meltwaters would have traversed Athabasca Valles in a few tens of hours (Keszthelyi et al., 2007). Later, this fluvial channel was covered with low viscosity lava that erupted from Cerberus Fossae (Jaeger et al., 2007). In summary, Cerberus Fossae is thought to be the surface expression of sub-surface dikes (fissure vents) that produced meltwaters and lavas in the last few percent of martian history.

It is known that dike emplacement can lead to graben subsidence (Rubin and Pollard, 1988; Rubin, 1993; Schultz et al., 2004) on both on Earth and Mars (Rubin, 1993). However, in addition to dike/fault-related subsidence, Head et al. (2003) suggested that the depressions along Cerberus Fossae had been formed by dike emplacement leading to melting-related subsidence. To enlarge the graben after dike emplacement, these authors invoked late-stage melting of the ice-saturated cryosphere adjacent to the dike. Head et al. (2003) suggest that melting and collapse are responsible for the majority of the observed subsidence. Evidence for subsidence related to collapse is suggested to exist in the form of chains of collapse pits associated with graben on Mars (Head et al., 2003; see Mege et al., 2003 for other examples). Head et al. (2003) suggest melting and subsequent subsidence of the surface, forms "late-stage pits and depressions". However, we note that Ferrill et al. (2004), studying analogues of martian collapse pits in Iceland, and modelling their formation in sandboxes, showed that collapse pits can form without melting in the case where dilatational faulting occurs at depth.

The above prompted us to study the detailed geometry of subsidence associated with Cerberus Fossae, to assess the relationships between fault-related subsidence, melting-related subsidence and possible dike emplacement.

## 3. Method

In order to investigate the evolution of the Northern Cerberus Fossae we have compiled data that quantifying graben lengths and throws. Images were collected that showed sufficient detail to enable graben lengths to be measured; these measurements were then matched with data constraining the vertical relief across the graben walls.

### 3.1. Datasets

MOLA, MOC, THEMIS and HiRISE data were used to construct a map, a DEM, photo-mosaics of the faults, and throw profiles.

To produce a photo-mosaic for initial mapping, we selected NASA Mars Global Surveyor (MGS) spacecraft's Mars Orbiter Camera (MOC) wide angle (WA) images (pixel width 240–270 m) (see Fig. 2a). Narrow angle (NA) images from the same instrument were selected to reveal the geometry of individual graben (Fig. 2b–n). All 27 MOC NA images of the NCF (pixel width 1.47–6.21 m) were examined which gave detailed coverage of <15% of the structures. 13 images were selected for Fig. 2 to show the correspondence between the MOC images and MOLA traverses. Additionally, THEMIS images from the NASA Mars Odyssey Mission spacecraft were selected to produce a high-resolution image mosaic (Fig. 4). This, when combined with high-resolution topographic data from MGS Mars Orbiter Laser Altimeter (MOLA), enabled characterisation of the map geometries and vertical offsets across the graben-bounding faults. THEMIS has two independent multi-spectral imaging subsystems: a 10-band thermal infra-red imager (IR) and a 5-band

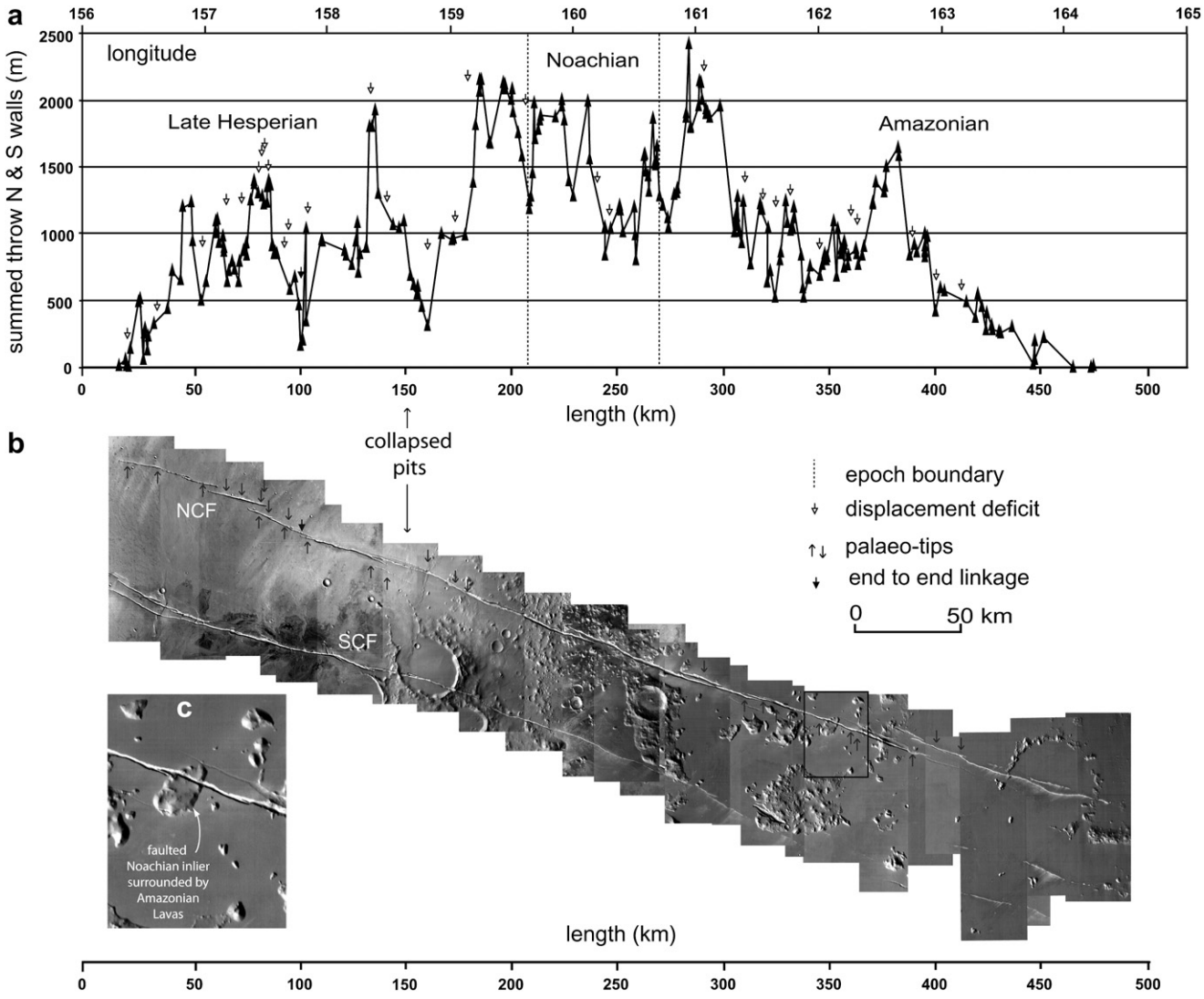


**Fig. 4.** Cumulative throw and length data summed across the strike of the Northern Cerberus Fossae. Data for the north and south walls are summed, but are symmetrically distributed between the north and south walls in most cases. (a) Northern Cerberus Fossae cumulative profile of length versus summed throw from MOLA data, showing positions of displacement deficits at the points of hard-linkage. (b) Positions of hard-linkage at the terminations of palaeo-tips on a THEMIS photo-mosaic. (c) Close-up of a Noachian inlier located in box on (b).

visible imager (VIS). Mainly IR daytime images, at a resolution of 100 m per pixel, were used in preparation of the mosaic. This mosaic was used to help position the MOLA data in map view. High-Resolution Imaging Science Experiment (HiRISE) images from the NASA Mars Reconnaissance Orbiter (MRO) have been studied to verify observations from other imagery.

To characterise vertical relief across graben walls, MOLA data profiles were studied. MOLA uses an IR laser 10 Hz pulse giving a ~168 m diameter footprint (e.g. Fig. 2o–w), with a centre-to-centre along-track footprint spacing of ~300 m along polar orbits (Smith et al., 2003), and a vertical resolution of about 1.5 m, in the relatively smooth area of the Elysium Planitia. Each footprint recorded latitude, longitude and height relative to the Mars datum. MOLA data were collected from February 1999 until the laser failed in June 2001. This resulted in uneven distribution of orbits along strike; all available data have been accessed for this study.

### 3.2. DEM and longitudinal graben profiles from MOLA data

Each Mars Global Surveyor spacecraft orbit that traversed the Northern Cerberus Fossae was accessed, and MOLA elevation data points between latitude 8°–12° north and longitude 156°–164.5° east were extracted from these orbits. From this matrix a DEM was produced showing the large-scale geometry of the Fossae (Fig. 1a). Further examination of the MOLA traverses and the neighbouring MOC images, showed that each fossa comprised a north wall and a south wall; there appear to be no half graben (e.g. Fig. 2). MOC NA, THEMIS and HiRISE images show that the graben sides are sub-vertical in their upper portions (see Fig. 2). Relevant data from 271 orbits were extracted giving, on further analysis, 1492 data points that constrain the elevation changes across the north and south walls of the graben (Fig. 1b–d). Fig. 2o–w shows examples of typical MOLA profiles across individual graben, showing the inherent uncertainty related to size and spacing of MOLA footprints. We used the maximum vertical difference between graben floors and the surrounding plains from 271 serial topographic sections to produce Fig. 1b–d in order to quantify the depth variation along the length of Northern Cerberus Fossae.

In Section 4 we argue that the vertical relief across the graben walls represents the throw across the graben-bounding fault because pre-existing topographic features have not been covered by sediment or disrupted by collapse during graben formation

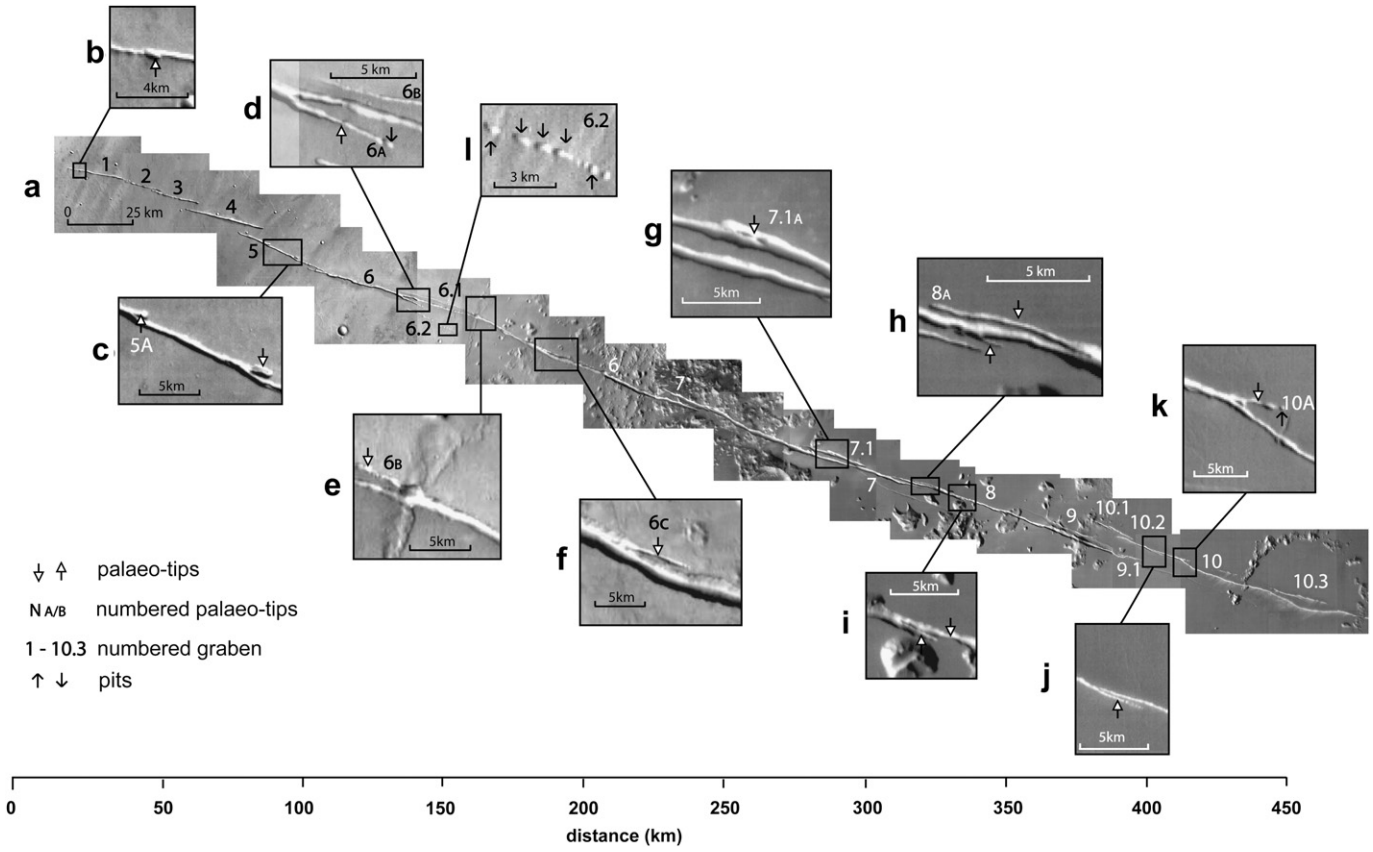


**Fig. 5.** THEMIS images of palaeo-tips along the Northern Cerberus Fossae located in Figs. 1 and 5. (a) THEMIS mosaic of the Northern Cerberus Fossae. (b)–(k) Enlarged THEMIS images to show positions of palaeo-tips, collapse pits and a pit chain.

(e.g. see Fig. 1b–d). For the rest of Section 3 we refer to vertical relief as throw, but the reader should bear in mind that this is an interpretation that we justify further in Section 4.

### 3.3. Topographic profiles across the graben matched to MOC images

To study how MOLA topographic traverses compare with detailed imagery of the graben, MOC NA images were located on our photo-mosaic maps (Fig. 2b–n) as were neighbouring MOLA profiles (Fig. 2o–w). Fig. 2 shows that the graben floor elevations, although averaged over the ~168 m diameter footprint of each MOLA footprint, are sampled by one or more individual MOLA data points. In places 2–3 MOLA footprints access the graben floor on a single traverse. Thus, we feel confident that the graben depths shown in Fig. 1b–c are representative of the actual depths, despite the ~168 m diameter footprint of each MOLA footprint. We used these data to assess whether the graben were infilled with sediment or disrupted by melting and collapse, and to study the mode of subsidence for the graben (see Section 4).

### 3.4. Matching MOLA data to individual graben

It is clear from both the DEM (Fig. 1) and the photo-mosaics (Figs. 2a and 4b) that the Northern Cerberus Fossae comprise a segmented array of graben. To obtain throw profiles for each constituent graben, we cross-correlated the MOLA coordinates and photo-mosaics to assign elevation data to particular graben. To achieve this, the latitude of each footprint from the north and south wall data set was plotted against longitude, and the resultant map was overlain on the THEMIS mosaic. This enabled matching of data to the particular graben identified on the mosaic. Thus, Fig. 3 shows both the map views and vertical relief (throw) across each graben. The lateral terminations of individual graben were defined where subsidence (throw) decreased to zero, and where graben traces coalesced along strike. We used this scheme to assess the growth and linkage history of each graben (see Section 4).

### 3.5. Identification of terrain from different epochs

In order to study the timing of graben formation, we prepared a geological map by cross-correlating between the DEM (Fig. 1) and THEMIS mosaic (Fig. 4). This enabled identification of terrain with different relative ages based on published crater densities. For example, the heavily cratered and higher topography of the Tartarus Montes (Noachian–Hesperian) was clearly older than the smoother, sparsely cratered Elysium Planitia (Amazonian). As the NCF cross-cut these terrains we hoped to ascertain whether the graben developed during or after formation of the cratered surfaces.

### 3.6. Identification of palaeo-tips and displacement minima

In order to study the detailed evolution of the surface traces of the graben, we mapped the terminations of graben and locations where graben coalesce or branch. Of particular interest here are small graben that branch off the main NCF graben, as seen in Fig. 5a–k. These structures resemble palaeo-tips (Cartwright et al., 1995; McLeod et al., 2000) that form when fractures/faults propagate along strike and link during the accumulation of displacement. This is known as hard-linkage in contrast to soft-linkage where fault ends overlap in map view, but remain separate. Such

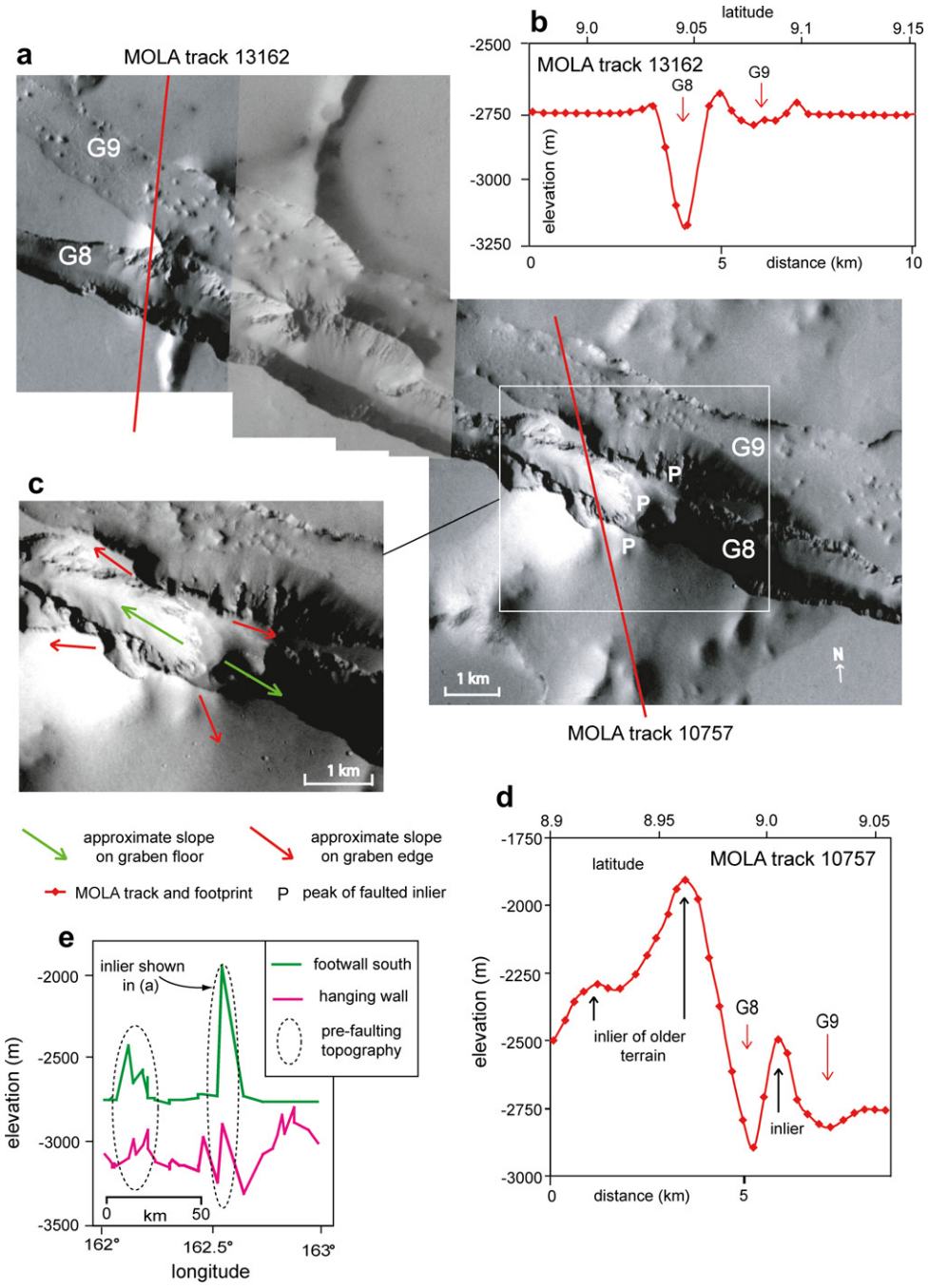


**Fig. 6.** Images of a faulted Noachian–Hesperian inlier along the Northern Cerberus Fossae. (a) Photo-mosaic of THEMIS visible wavelength images from west to east, V10829011, V10205009, V22797022 and V01979006. Graben 8 (G8) cross-cuts and displaces the older Graben 9 (G9), and a Noachian to Early Hesperian inlier (peak P). (b) MOLA traverse 13162 showing topographic cross sections of G9 and the more recent G8. (c) Detail of interpreted slopes associated with the faulted inlier. (d) MOLA traverse 19757 showing a profile across G8 and G9 in relation to the offset older terrain. (e) An extract from Fig. 1c showing the along strike topographic offset across the faulted Noachian inlier.

palaeo-tips occur beyond the point of linkage, and thus indicate the existence of former en-echelon structures, where a relay zone has become breached by subsequent displacements. We are interested in these palaeo-tips because analysis of displacements associated with them can reveal incremental growth of the structures in question. For example, the positions where en-echelon structures existed in the past are commonly the sites of displacement deficits. Deficits develop because there is no structure to accommodate displacement early in the faulting (Dawers et al., 1993; Mansfield and Cartwright, 2001). Displacements only accumulate after en-echelon tips propagate and eventually link.

To assess whether throw deficits exist at the locations of palaeo-tips, a cumulative throw profile was constructed by summing the maximum throw values across the NCF and plotting them against length (Fig. 4a). Then, palaeo-tips were identified on the THEMIS mosaic (Fig. 4b) and their locations were compared with the throw deficits in the cumulative profile.

### 3.7. Calculation of breaching indices

To assess how the graben developed through time, palaeo-tips were identified on the THEMIS mosaic Fig. 4b, and cross-correlated

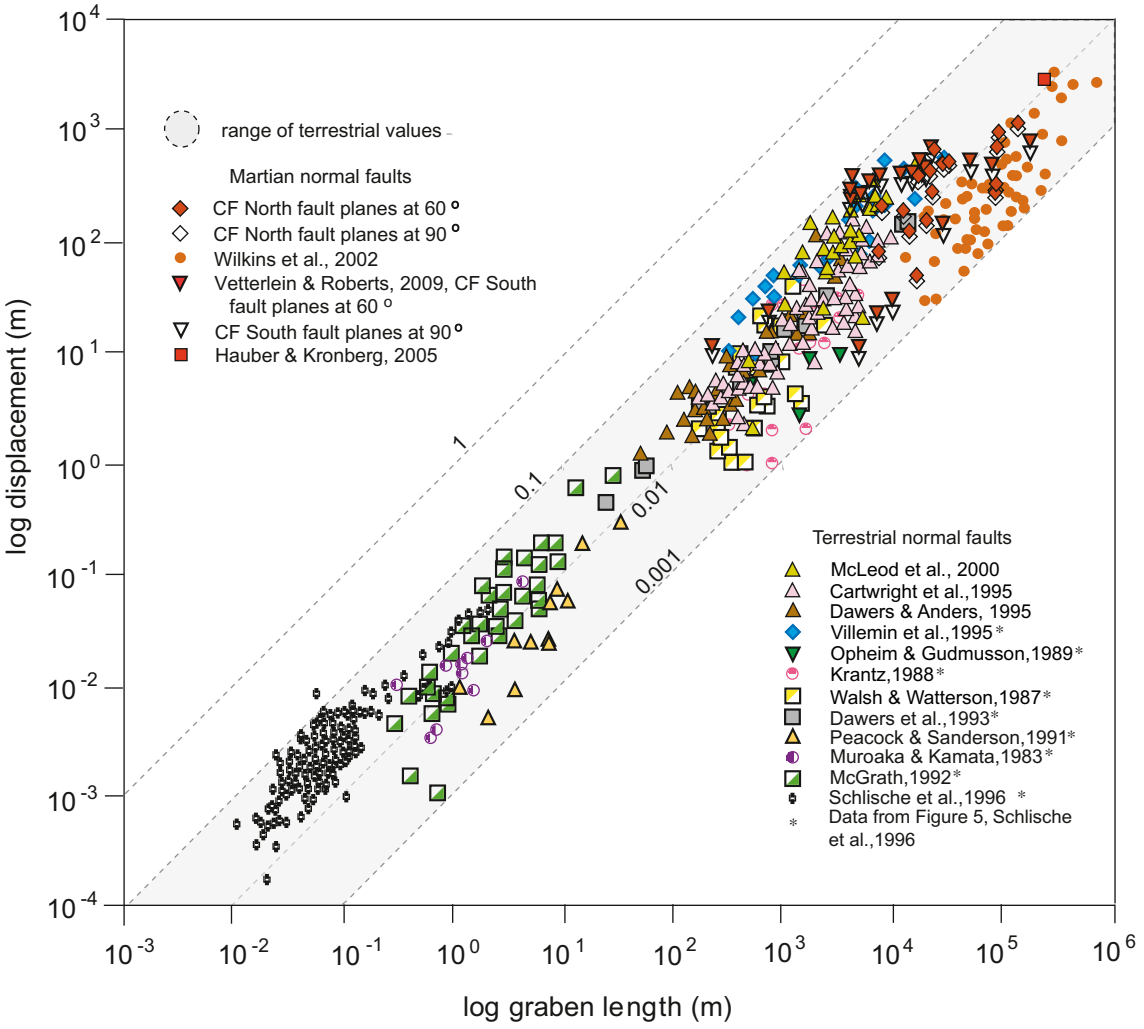


**Fig. 7.** Comparison of throw/length ratios of the north and the south walls of individual graben of the Northern Cerberus Fossae, both at 90° and 60°, with other martian and terrestrial normal faults, some after Schlische et al. (1996). Shaded area represents range of terrestrial normal fault values.

with throw deficits in the cumulative throw/length profile (Fig. 4a). Of the 31 palaeo-tips that were identified, there were sufficient MOLA data from 7 to calculate breaching indices (see Fig. 3a) using the equation of Cartwright et al. (1995). The throw on the palaeo-tip stops accumulating at the time of hard-linkage to the adjacent graben. Thus, by dividing the throw on the palaeo-tip by the throw on the adjacent linked graben, one can calculate a relative age for linkage, expressed as a percentage of the total throw on the adjacent graben, assuming constant throw-rates through time.

Breaching indices (BIs) are calculated thus:-

$$BI = TP/TG \times 100 \quad (1)$$

where TP is the throw on palaeo-tip, and TG is the throw on adjacent linked graben (after Cartwright et al., 1995).

### 3.8. Comparison of data with those from other graben

To assess similarities and differences with other graben, we compared throw/length values of the north and south walls of individual NCF graben with data from other martian and terrestrial normal faults (Fig. 7). We also compared slip-rate data for terrestrial normal faults with throw-rates implied by offsets for Graben 1, 6, 8 and 10, given the range of proposed dates since the onset of faulting namely 200 Ma, 100 Ma, 50 Ma, 10 Ma and 1.5 Ma (Fig. 8); this range exists because of the inherent uncertainty in crater counting ages.

## 4. Results

The DEM (Fig. 1a) shows the Northern Cerberus Fossae cross-cutting terrain of three different ages. In the west, the NCF offset Late Hesperian/Early Amazonian lavas that are 3.2–2.0 Ga in age (Hartmann and Neukum, 2001), whilst older Early Noachian to Early Hesperian rocks, with an age range 4.1–3.5 Ga (Hartmann, 2005; Hartmann and Neukum, 2001), are offset in the central portion of the NCF. In the east, extremely young Amazonian rocks are offset, with crater count ages implying that displacements post-date 200 Ma to <10 Ma (see Section 2). The displacement of 200 to <10 Ma Amazonian terrain indicates formation of the Northern Cerberus Fossae in the last few percent of Martian history.

The along strike elevation profiles in Fig. 1b–d provide insights into the age of the initiation of faulting relative to the cratered surfaces, the extent of vertical motions, and the existence of pre-faulting topography. Vertical offsets between the footwalls and hangingwalls of the faults achieve values of up to 1156 m, decreasing along strike as hangingwall subsidence becomes zero at ~156.3°

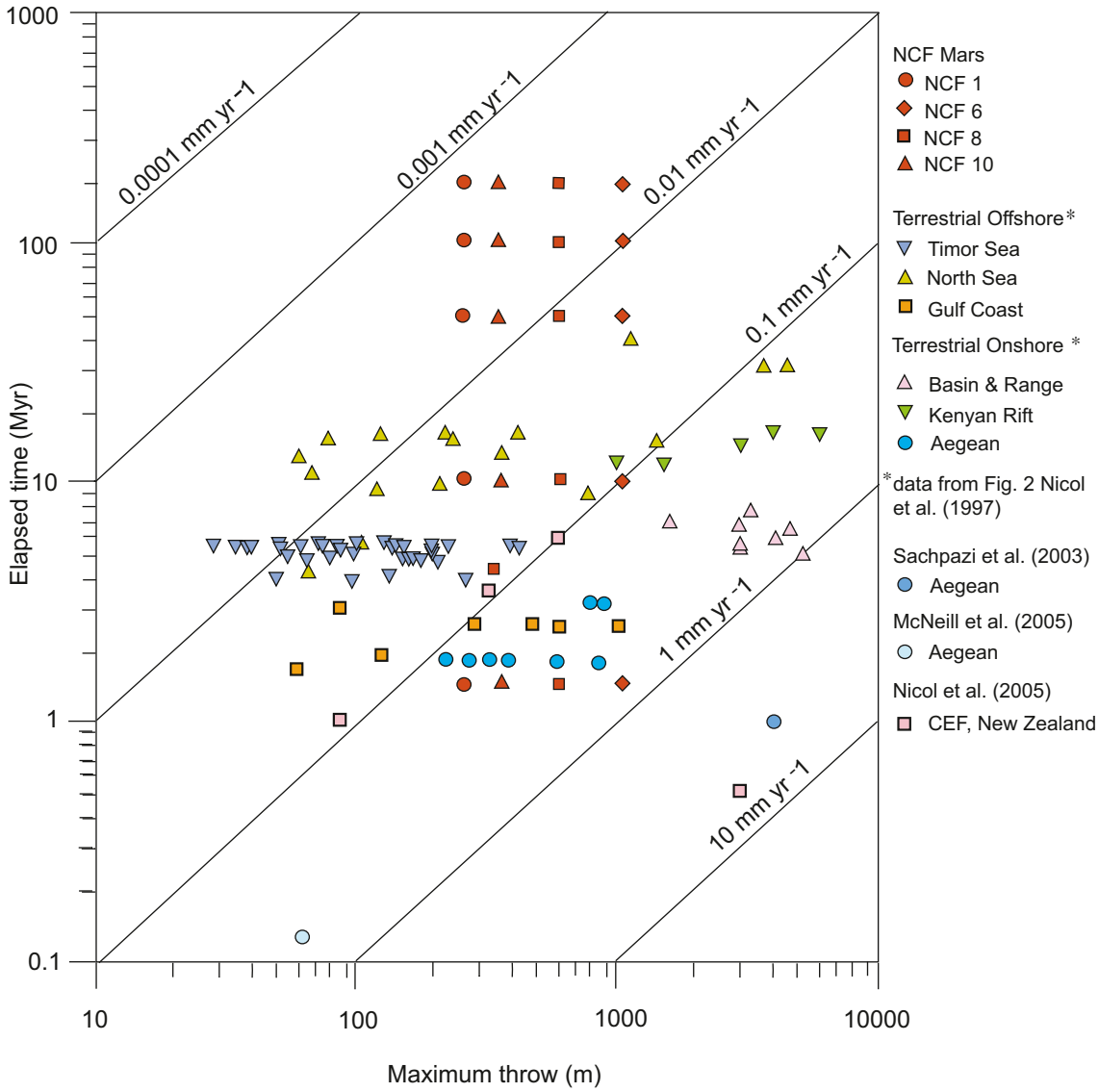


**Fig. 8.** Plot of elapsed time since the onset of faulting versus maximum throw for individual graben from the Northern Cerberus Fossae and terrestrial normal faults. Terrestrial data from Nicol et al. (2005). Data for the NCF are from this study. Data from 4 representative NCF graben have been plotted, with implied deformation rates if the throws have developed in 200 Myrs, 100 Myrs, 50 Myrs, 10 Myrs and 1.5 Myrs.

and ~164.4° longitude (Fig. 1b–c); this is evident when examining offsets across both the north wall (Fig. 1b) and south wall (1c). The topographic profiles for the footwalls in Fig. 1 have a number of peaks and troughs. The same peaks and troughs can be identified on the north and south footwalls (Fig. 1d). Cross-correlation with the MOLA DEM and the THEMIS photo-mosaic (Figs. 1a, 4b and 5a) reveals that these peaks and troughs are topography associated with crater rims and Noachian inliers that pre-date the faulting (e.g. Figs. 4c and 6a). Of interest here is that the peaks and troughs can also be identified on the floors of the graben (this is indicated by the ellipse shapes on Fig. 1b and c). Our interpretation is that pre-faulting topography has been offset by faulting and downthrown. Preserved topography on the graben floors include features from the Late Hesperian Elysium lavas, the Noachian Tartarus Montes, Amazonian landforms and Noachian inliers (Fig. 1). An example of such faulted Noachian topography on a graben floor can be seen in the THEMIS image in Fig. 6 (located in Figs. 1 and 5). A Noachian inlier, surrounded by Amazonian lavas has been offset by faulting and downthrown. The topographic peak of the inlier, P, is clearly preserved on the floor of the graben (G8), and the topography is quantified in Fig. 6e which presents a MOLA traverse across the structure. These observations of pre-faulting topography preserved on the floor of the graben demonstrate that (1) infill by post-faulting material has not blanketed and obscured the pre-existing topography, (2) cryospheric melting and collapse was not of sufficient magnitude to destroy such features. The smallest topographic feature that we have identified both on the floor of a graben and on the footwall is only 30 m high, implying that sediment infill is less than a few tens of metres, at least at this location (Fig. 1b topography detail box).

Thus, we interpret the changes in elevation across the graben walls (Fig. 1b–c) as preserved faulted offsets (throws) and not fault offsets minus a significant value for sediment infill.

In order to reveal the spatial resolution of throw measurements, we prepared Fig. 2 which shows how MOLA topographic data relate to features seen in high-resolution imagery (MOC images). It is clear that the MOLA footprints are much smaller than the graben widths, suggesting that they provide a reliable estimate of the

depth profiles across the graben. This is confirmed by corresponding MOC NA images (Fig. 2b–n); these show double graben where the MOLA data suggest double graben, and overall the MOLA profiles resemble the graben shown on the MOC images. Thus, we are confident that the vertical offset profiles across the graben shown in Fig. 1b and c are an acceptable representation of the true vertical offset variations.

Considering the overall throw profile for the Northern Cerberus Fossae (Fig. 1b–c and Fig. 4, which is derived from the same data set as Fig. 1b–c), throws are greatest in the centre of the Northern Cerberus Fossae, a feature that is common for fault systems on the Earth (Walsh and Watterson, 1988; Dawers et al., 1993; Cowie and Roberts, 2001). The throw profile in Fig. 4a resembles that for a single fault system on the Earth in that (1) throws are greatest in its central portion, (2) its throw/length ratio is 2000/450 000, that is, 0.004, with a range of terrestrial values falling between 0.001 and 0.1 (Fig. 7). Thus, the vertical relief across the graben is not too great to explain solely with faulting. Faulting is a plausible explanation for the observed subsidence values and this is one reason why there is no need to invoke melting and collapse to form these graben.

To investigate when faulting and graben formation started we compared throws where the graben cross different ages of terrain (Figs. 1b–c and 4a). The vertical offsets do not increase dramatically across the boundary between the older Noachian rocks and younger Amazonian rocks. Offsets of late Hesperian rocks are comparable to those for Amazonian rocks. The maximum cumulative throw is located within the youngest Amazonian terrain. If faulting had been ongoing in the Hesperian and Noachian, rocks of these ages would display greater throws than younger Amazonian rocks; Fig. 4a shows that this is not the case. Our interpretation is that the displacements were not accumulating before formation of the Amazonian rocks and that all throws post-date formation of the Amazonian rocks dated by crater counting; the faulting is thus very young (<200–10 Ma).

The overall throw profile in Fig. 4 is serrated with a number of maxima and minima along strike. On Earth such serrated profiles are commonly explained as the result of the linkage of precursor fault segments (McLeod et al., 2000; Lohr et al., 2008). To investigate how throws vary in relation to the segmented map traces of the graben, we examined throw values near locations of en-echelon graben and at locations where palaeo-tips indicate hard-linkage between precursor en-echelon graben.

First, we note that locations with subsidence minima in the HW traces in Fig. 1b and c (light blue arrows) correspond to identifiable locations of en-echelon graben revealed by the MOC and THEMIS photo-mosaics (Figs. 2 and 4b). On Fig. 1, at ~40 km along strike from the western end, Graben 1 and 2 show an en-echelon offset (arrow 1), at ~110 km Graben 5 and 6 show an en-echelon offset (arrow 2), and, at blue arrow 3, at ~320 km, there is an en-echelon offset between Graben 7 and 8. These shallow points for the overall graben floor are clearly structurally controlled showing that graben fault-trace geometries correlate with fault throws. Subsidence due to fault activity can explain these features and this is another reason why there is no need to appeal to subsidence related to melting and collapse.

Second, we note that NCF can be divided into ten main graben, with one large, and at least six smaller parallel graben (Fig. 3b), revealed by profiles of vertical offset along each individual graben. Graben located centrally along the fault array, such as Graben 6 and 7 have larger offsets than those located at the ends of the array (Fig. 3). This pattern, where centrally-located faults have higher displacements than distally-located faults is typical of fault systems on the Earth (Dawers and Anders, 1995; McLeod et al., 2000; Cowie and Roberts, 2001; Roberts and Michetti, 2003; Papanikolaou and Roberts, 2007). Throw/length ratios for individual graben are in the range 0.1–0.001, similar to those on the Earth (Fig. 7). Throw gradients near the tips of the Northern Cerberus Fossae graben are 5–1.5% for the north and south walls separately (Fig. 3a). These compare with terrestrial tip gradients of 10–5% (Cowie and Shipton, 1998; Cartwright and Mansfield, 1998; Roberts and Michetti, 2003). Again, subsidence due to fault activity can explain these features with no need to invoke subsidence related to melting and collapse.

Third, we note that in detail, individual graben have serrated offset profiles. For example, in Fig. 3a Graben 6 has a lower offset portion located at 200 km along strike, between two higher offset portions located 180 km and 220 km along strike. At the location of this displacement deficit, a smaller graben (Graben 6C) is truncated by the main graben (Graben 6). This is interpreted as a palaeo-tip, where two graben have linked along strike. Our interpretation is that the displacement deficit has been preserved because the site was formerly an en-echelon relay zone between offset graben with no faulting accumulating at this point prior to linkage. Palaeo-tips with associated displacement deficits are a common feature of the other graben. For example Graben 8 shows a displacement deficit at ~315 km along strike between highs at 305 km and 325 km, the low point corresponding to the location where hard-linkage has isolated Graben 8A (now PT 8A). Indeed, Fig. 4 demonstrates that most if not all of the 31 palaeo-tips identified on the THEMIS mosaic are associated with throw deficits. These throw deficits are clearly controlled by the fault evolution and again there is no need to appeal to subsidence related to melting and collapse.

In order to assess the relative timing of palaeo-tip formation events for different examples, breaching indices were calculated, assuming constant throw-rates through time (see Section 3.8). As can be seen from the values in the breaching indices boxes in Fig. 3a, Palaeo-tip 10A, with a BI of 20%, was the earliest example of hard-linkage to a larger graben that we have been able to constrain, an event which happened when only 20% of the total slip on Graben 10 had accumulated. Palaeo-tips 5A (BI 30%), 6B (BI 33%) and 6C (BI 26%) also hard-linked relatively early, when only between a quarter and a third of the total observed throw of Graben 5 and 6 had accumulated, assuming a constant throw-rate through time. Palaeo-tips 7.1A (BI 92%), 8A (BI 92%) and 6A (BI 99%) were the most recent breaching events, occurring within the last 10% of throw accumulation at these locations. The significance of these breaching index values is not the precise values, as clearly the calculation involves a significant assumption, that is, that throw-rates were constant though time, and it is well-known that points of linkage are places where throw-rates are likely to change (Cowie and Roberts, 2001). Rather, the significance of the values is that hundreds to thousands of metres of throw are likely to have accumulated between the times of linkage at different sites. This reveals an incremental addition of displacement to the fault system through time with concomitant and diachronous graben linkage along strike. Coseismic throws for earthquakes on the Earth are ~ 1m for a Ms 6.5 earthquake with an along strike rupture length of ~15–20 km (Wells and Coppersmith, 1994), and Ms 6.5 earthquakes are separated in time by hundreds to thousands of years given extension rates of a few millimetres per year (Cowie and Roberts, 2001). If similar relationships exist on Mars, it would have taken millions of years to accumulate throws of hundreds to thousands of metres (Wilkins et al., 2002). Thus, the graben would have formed over millions of years, rather than forming in a single melting/collapse event.

The existence of collapse pits has been used to postulate subsidence through melting/collapse (Head et al., 2003). Our data allow such features to be viewed in relation to the overall subsidence associated with the Northern Cerberus Fossae. The most

prominent collapse pits are shown in Fig. 5d and l, at about 150 km from the western end of the graben system we have studied. The pits occur where overall subsidence (throw) is as low as ~300 m (Fig. 4), in a zone which was a soft-linked relay zone until breaching occurred very late in the faulting history (Breaching Index of 99; Fig. 3). We suggest that subsidence associated with these pits is relatively minor compared with the ~500–1000 m of subsidence that exists within 50 km to the west and east of this location. We interpret the pits as the initial phase of subsidence that occurs at points of graben linkage. Note that this "initial stage" may be late in the faulting history (see Head et al., 2003; "late-stage pits and depressions") as linkage occurred very late at this location, within the last few percent of the faulting history. In any case, Ferrrill et al. (2004) have shown that such pits can form in the absence of melting cryosphere in sandbox model experiments; thus, we suggest the pits cannot be used to conclude that melting/collapse is the dominant subsidence mechanism.

We note that one graben has a rather subdued topographic expression (Graben G9 in Fig. 6a). On Earth it is not unusual to find faults of different ages and at different stages of evolution in an area of extension. Graben 9, which has been included in this study, and an unmarked graben south of Graben 7 and 8, (which has not as there are no defining MOLA data) show evidence from the THEMIS images and, in the case of Graben 9, a MOLA cross section (Fig. 6b), of a more subdued relief than other graben of similar length (Fig. 3). We suggest Graben 9 may represent an earlier stage of graben formation with a consequently longer time for sediment and/or lava to accumulate on the floor, but clearly this needs more data and study. Graben 9 has been cross-cut by Graben 8, which is younger, deeper, with well-defined sides (Fig. 6a).

Finally, we assess the likely deformation rates for the graben. The throws documented in Figs. 1, 3 and 4 can be combined with the age-ranges of the offset cratered surfaces to gain estimates of throw-rates. If the onset of faulting was 200 Ma, throw-rates for four of the graben range from 0.0014 mm/year for Graben 1 to 0.006 mm/year for Graben 6 (Fig. 8). This is likely to be an underestimate of the throw-rates as 200 Ma is the maximum age assigned for the youngest faulted Cerberus lavas. If faulting post-dated one of the youngest proposed ages, 1.5 Ma, the throw-rates would be, at least, in the range from 0.18 to 0.73 mm/year (Fig. 8). Thus, throw-rates in the range of 0.0014–0.73 mm/yr are implied by the throw values we report given the range on crater count ages. All these throw-rates fall within terrestrial ranges (Fig. 8). Thus, we suggest that such rates are not unreasonable given that similar values have been recorded on the Earth.

## 5. Discussion

The observations in this paper show that subsidence along Northern Cerberus Fossae appears to be associated with geometries that resemble fault systems from the Earth. Specifically, subsidence occurs across segmented faults that show en-echelon and end-on geometries associated with displacement deficits. The faults have similar throw/length ratios and tip gradients to those on Earth, and crater count ages for the offset surfaces suggest deformation rates that are similar to those documented on the Earth. These observations have implications for mechanism that formed Cerberus Fossae.

Suggested that subsidence associated with Cerberus Fossae was dominated by collapse following crysospheric melting produced by dike intrusion. However, we have shown that pre-existing topography is preserved on the graben floors. This would be an unlikely outcome if the graben floors had undergone subsidence and collapse due to melting or if the graben walls had collapsed inwards during melting. We suggest that the preservation of pre-existing topography on graben floors is a result of subsidence of rigid blocks due to faulting. We also observe palaeo-tips to graben. These features reveal that subsidence was incremental, with early graben geometries evolving via segment linkage to form the present-day geometry over a time period that was probably on the order of millions of years. These palaeo-tips are associated with deficits in graben subsidence. Deficits also exist where graben are soft-linked across en-echelon relay zones along Cerberus Fossae. We see no reason why cryospheric melting would produce such geometries. Rather, such geometries are characteristic of fault-related subsidence on the Earth where no cryospheric melting has occurred (e.g. Cartwright et al., 1995; Dawers and Anders, 1995; McLeod et al., 2000; Lohr et al., 2008; Podolsky and Roberts, 2008). Deficits form where linkage post-dates displacement accumulation along neighbouring faults so that the point of linkage has accrued displacement for a shorter period of time than the neighbouring faults. Some evidence exists for minor collapse related subsidence in the form of pit chains. However, these are located where overall subsidence is minor. In any case, such collapse is not necessarily associated with melting (Ferrrill et al., 2004). Thus, the presence of collapse pits associated with the NCF cannot be used as direct evidence for melting. We interpret the collapse pits as the early stage of graben subsidence because they are located at a site where recent linkage between two previously-separate graben has occurred.

If faulting is responsible for that majority of subsidence, as we argue above, then we hypothesize that the subsidence must have taken millions of years to form. This conclusion must follow if faulting on Mars involves marsquakes where the relationships between magnitude, rupture length and coseismic throw are not different to those on the Earth by values approaching an order of magnitude. Wells and Coppersmith (1994) show that on Earth, throws in even the largest magnitude earthquakes with rupture lengths of tens to hundreds of kilometres are in the order of ~1–20 m. If the same is true for Mars, the ~1000 m throws across the largest graben within the Northern Cerberus Fossae (Graben 6 is ~150 km in length) would have formed in hundreds to thousands of marsquakes. We suggest that the fact that faults in Northern Cerberus Fossae exhibit similar throw/length ratios to those on Earth (Fig. 7) argues that the relationship between coseismic throw and coseismic rupture length is unlikely to be drastically different on Earth and Mars (note that Schultz et al., 2006 suggest that throw/length relationships on Mars are less than an order of magnitude different to those on Earth, stating that the difference is about a factor of 5). This is the basis for our hypothesis that Northern Cerberus Fossae would have formed in hundreds to thousands of metre-scale slip events, if slip events this large were involved. With respect to the timing of such slip events (marsquakes), extension rates across presently active normal fault systems on Earth, whose lengths are in the region on hundreds of kilometres, and are known to generate large magnitude earthquakes (>Ms 6.0), are in the range of ~0.001–10 mm/yr (Cowie and Roberts, 2001). These rates are comparable to those implied by offsets of cratered surfaces around Northern Cerberus Fossae (Fig. 8). If such deformation rates are correct for Northern Cerberus Fossae (~450 km length), recurrence intervals for large magnitude marsquakes (slip events of a few metres) would have been hundreds to thousands of years. It remains to be seen if the structures are still active, but as mentioned above, crater count ages for lava surfaces offset across Cerberus Fossae imply activity in the last few percent of martian history.

The significance of the above is that for subsidence formed by faulting over millions of years, the internal volume of the graben need not show a relationship with the volume of meltwater released in a few hours to days to form a catastrophic flood like that which is thought to have formed Athabasca Valles (Fig. 1).

It is unclear to us whether the faulting we interpret was driven by dike intrusion or simply due to dilational faulting (Mege et al., 2003; Ferrrill et al., 2004). Ferrrill et al., 2004, used analogue sandbox models to produce faults with similar geometries to those we describe in NCF without melting. However, Head et al. (2003) provide photographic evidence from a MOC image of what may be an exposed dike on the floor of one graben (their Fig. 2c), and Cerberus Fossae is radial to Elysium Mons volcano, an orientation that suggests faulting above a dike(s). This clearly needs further study. Future work should attempt to quantify the relationship between subsidence, faulting, melting and melt-water discharge for the South Cerberus Fossae, where the existence of Athabasca Valles has prompted hypotheses linking such variables.

## 6. Conclusions

Observations of MOC, THEMIS and HiRISE images, and MOLA data can be used to document spatial variations in vertical offset along the NCF, a system of graben cross-cutting the youngest surface on Mars. Our results show the following.

1) The NCF is a linear segmented array of graben cross-cutting terrain of different ages ranging from Early Noachian to the most recent Late Amazonian.
2) Subsidence is largest in the middle of its surface trace ($\sim$1000 m), decreasing to zero along strike at its terminations, with the largest offsets for Amazonian surfaces.
3) Pre-faulting topography can be identified on the graben floor suggesting that the subsidence is due to faulting rather than melting and collapse. The subsidence profile is thus a fault throw profile that resembles those for single fault systems on the Earth.
4) Deficits in subsidence produced by fault throw occur where graben are arranged en echelon, or where graben have linked along strike isolating palaeo-fault tips, consistent with the hypothesis that subsidence is fault controlled.
5) Throw/length ratios for the overall Northern Cerberus Fossae and individual graben are within the range of 0.0–0.001, similar to those for faults on the Earth, supporting the hypothesis that they formed through the cumulative effect of repeated slip events with a similar coseismic throw to length ratio as those measured on the Earth (e.g. Wells and Coppersmith, 1996).
6) The throw is not greater where the faulting offsets older terrain, suggesting that faulting initiated after 200–$<$10 Ma.
7) Throw-rates implied by crater count ages of offset surfaces are in the range of 0.0014–0.73 mm/yr, similar to those for fault systems of similar dimensions on the Earth.
8) If subsidence occurred through the cumulative effect of coseismic throws with throw/length relationships similar to those on the Earth, the deformation rates implied by crater counts would imply faulting developed over millions of years rather over the timescale of a single dike emplacement episode.

## Acknowledgements

We thank John Guest, Ian Crawford, Louise Bishop and Dominic Fortes for discussions concerning this study and Thomas Dewez for help with constructing the DEM. We thank Joe Cartwright and Richard Schultz for their detailed reviews. This study was partly funded by Birkbeck College, and benefited from provision of the Regional Planetary Imaging Facility at UCL.

## References

Berman, D.C., Hartmann, W.K., 2002. Recent fluvial, volcanic and tectonic activity on the Cerberus Plains of Mars. Icarus 159, 1–17.
Burr, D.M., McEwen, A.S., Sakimoto, S.E.H., 2002. Recent aqueous floods from the Cerberus Fossae. Mars. J. Geophys. Res. 29, 1–4. 1, 1029/2001GLO13345, 13.
Cartwright, J.A., Mansfield, C.S., 1998. Lateral displacement variation and lateral tip geometry of normal faults in the Canyonlands National Park, Utah. J. Struct. Geol. 20, 3–19.
Cartwright, J.A., Trudgill, D.B., Mansfield, C.S., 1995. Fault growth by segment linkage: an explanation for the scatter in maximum displacement and trace length data from the Canyonlands Grabens of SE Utah. J. Struct. Geol. 17 (9), 1319–1326.
Cowie, P.A., Roberts, G.P., 2001. Constraining slip rates and spacings for active normal faults. J. Struct. Geol. 23, 1901–1915.
Cowie, P.A., Shipton, Z.K., 1998. Fault tip displacement gradients and process zone dimensions. J. Struct. Geol. 20, 1075–1087.
Dawers, N.H., Anders, M.H., 1995. Displacement-length scaling and fault linkage. J. Struct. Geol. 17 (5), 607–614.
Dawers, N.H., Anders, M.H., Scholtz, C.H., 1993. Fault length and displacement: scaling laws. Geology 21, 1107–1110.
Ferrrill, D.A., Wyrick, D.Y., Sims, D.W., Franklin, N.M., 2004. Dilational fault slip and pit chain formation on Mars. GSA Today 14 (10), 4–12. doi:10.1130/1052-5173.
Fuller, E.R., Head III, J.W., 2002. Amazonis Planitia: the role of geologically recent volcanism and sedimentation in the formation of the smoothest plains on Mars. J. Geophys. Res. 107 (E10), 5081.
Hartmann, W.K., Berman, D.C., 2000. Elysium Planitia lava flows: crater count chronology and geological implications. J. Geophys. Res. 105, 15011–15026.
Hartmann, W.K., Neukum, G., 2001. Cratering chronology and the evolution of Mars. Space Sci. Rev. 96 (1–4), 165–194.
Head, J.W., Wilson, L., Mitchell, K.L., 2003. Generation of recent massive water floods at the Cerberus Fossae, Mars by the dike emplacement, cryospheric cracking, and confined aquifer groundwater release. Geophys. Res. Lett. 30 (11), 1577. 31 1–4.
Jaeger, W.L., Keszthelyi, L.P., McEwen, A.S., Dundas, C.M., Russel, P.S., 2007. Athabasca Valles, Mars: a lava draped channel system. Science 317 (1709). doi:10.1126/science.1143315.
Keszthelyi, L.P., Denlinger, R.P., O'Connell, D.R.H., Burr, D.M., 2007. Initial insights from 2.5D hydraulic modelling of floods in the Athabasca Valles, Mars. Geophys. Res. Lett. 34, L21206. doi:10.1029/2007GL031776.
Lohr, T., Krawczyk, C.M., Oncken, O., Tanner, D.C., 2008. Evolution of a fault surface from 3D attribute analysis and displacement measurements. J. Struct. Geol. 30, 690–700.
Mansfield, C., Cartwright, J., 2001. Fault growth by linkage: oservations and implications from analogue models. J. Struct. Geol. 23, 745–763.
McEwen, A.S., Preblich, B.S., Turtle, E.P., Artemieva, N.A., Golombek, M.P., Hurst, M., Kirk, R.L., Burr, D.M., Christensen, P.R., 2005. The rayed crater Zunil and interpretations of small impact craters on Mars. Icarus 176, 351–381.
McKenzie, D., Nimmo, F., 1999. The generation of martian floods by the melting of ground ice above dykes. Nature 397, 231–233.
McLeod, A., Dawers, N.H., Underhill, J.R., 2000. The propagation and linkage of normal faults: insights from the Strathspey – Brent – Statfjord fault array, northern North Sea. Basin Res. 12, 263–284.
Mege, D., Cook, A.C., Garel, E., Lagabrielle, Y., Cormier, M.-H., 2003. Volcanic rifting in Martian grabens. J. Geophys. Res. 108 (E5), 5041.
Nicol, A., Walsh, J., Berryman, K., Nodder, S., 2005. Growth of normal faults by accumulation of slip over millions of years. J. Struct. Geol. 27, 327–342.
Papanikolaou, I., Roberts, G.P., 2007. Geometry, kinematics and deformation rates along active normal fault system in the southern Apennines: implications for fault growth. J. Struct. Geol. 29, 166–188.
Plescia, J.B., 2003. Cerberus Fossae, Elysium, Mars: a source for lava and water. Icarus 164, 79–95.
Podolsky, D.M.V., Roberts, G.P., 2008. Growth of the volcano-flank Koa'e Fault System, Hawaii. J. Struct. Geol. 30, 1254–1263. doi:10.1016/j.jsg.2008.06.006.
Roberts, G.P., Michetti, A.M., 2003. Spatial and temporal variations in growth rates along active normal fault systems: an example from the Lazio-Abruzzo Apennines. Cent. Italy. J. Struct. Geol. 26, 339–376.
Rubin, A.M., Pollard, D.D., 1988. Dike-induced faulting in rift zones of Iceland and Afar. Geology 16, 413–417.
Rubin, A.M., 1993. Dike-induced faulting and graben subsidence in volcanic rift zones. J. Geophys. Res. 97 1939–1858.
Schlische, R.W., Young, S.S., Ackermann, R.V., Gupta, A., 1996. and Figure 5a references therein Geometry and scaling relations of a population of very small rift-related normal faults. Geology 24 (8), 638–686.
Schultz, R.A., Okubo, C.H., Wilkins, S.J., 2006. Displacement-length scalingrelations for faults on the terrestrial planets. J. Struct. Geol. 28, 2182–2193.
Schultz, R.A., Okubo, C.H., Goudy, C.L., Wilkins, S.J., 2004. Igneous dikes on Mars revealed by Mars Orbiter laser altimeter topography. Geology 32 (10), 889–892.
Smith, D.E., Neumann, G.A., Ford, P.G., Arvidson, R.E., Guinness, E.A. and Slavney, S., 2003. MGS Laser Precision Instrument Experiment Data Record. MGS-M-MOLA-3-PEDR-L1A-V1. 0, NASA Planetary Data System.
Tanaka, K.L., Skinner, J.A. and Hare, T.M., 2005. Geologic Map of the Northern Plains of Mars. Pamphlet to accompany Scientific Investigations Map 2888, USGS for NASA.

Vaucher, J., Baratoux, D., Pinet, P.C., Mangold, N., Ceuleneer, G., Gregoire, M., Daydou, Y., Chevrel, S., Neukum, G., the HRSC Co-Investigator Team, 2006. Cerberus Plains, Mars: chronology of volcanic event and evidence of recent tectonic activity. Lunar Planetary Sci. (XXXVII).

Walsh, J.J., Watterson, J., 1988. Analysis of the relationship and dimensions of faults. J. Struct. Geol. 10, 239–247.

Wells, D.L., Coppersmith, K.J., 1994. New empirical relationships among magnitude, rupture length, rupture width, rupture area and surface displacement. Bull. Seismolog. Soc. Am. 84, 974–1002.

Wilkins, S.J., Schultz, R.A., Anderson, R.C., Dohm, J.M., Dawers, N.H., 2002. Deformation rates from faulting at the Tempe Terra extensional province. Mars. Geophys. Res. Lett. 29 (18), 1884. doi:10.1029/2002GL01591.